Kinematic Synthesis of a Tendon-Driven 4R Planar Robotic Arm

Chiara Lanni(✉), Giorgio Figliolini, and Michele D'Angelo

Department of Civil and Mechanical Engineering, University of Cassino and Southern Lazio, Cassino, Italy
lanni@unicas.it

Abstract. This paper deals with the kinematic synthesis of a tendon-driven 4R planar robotic arm with 4-d.o.f.s and thus, two times redundant, which behavior is that of a deployable mechanism with wide workspace and small volume, when fully closed. The kinematic synthesis of the proposed 4R planar robotic arm has been developed by superposing three tendon-driven kinematic chains, in order to operate by means of a remote actuation, the last three links, since the first link is actuated directly. Moreover, a suitable algorithm has been formulated to operate the proposed 4R robotic arm in order to reach a given target point within the working area, as well as, to move inside a narrow environment in order to get a given configuration of the robotic arm. Examples are reported to simulate and test the working of the proposed robotic arm in different operating conditions.

1 Introduction

Tendon-driven redundant robots are used in many fields for accessing harsh and confined environments that can be inaccessible or dangerous for the human beings. As stated by Tsai (1995, 1999), along with Tsai and Lee (1989), these serial robots are characterized by the following main advantages: 1) All actuators can be installed on the fixed base, resulting in a compact and lightweight design; 2) A well-designed tendon transmission system has little backlash. When these serial robots are also redundant, they can be considered deployable mechanisms, since characterized by wide workspace and small volume, when fully closed.

Articulated tendon-driven robotic mechanisms were also investigated by Figliolini and Ceccarelli (1998), Krovi et al. (2002) and Uyguroglu and Demirel (2006). Ozawa et al. (2014) suggested a classification and design of tendon driven mechanisms, while Londi et al. (2004) and Okur et al. (2015) developed a control system. A tendon-driven robotic arm to remove skins by wine fermentation tanks was designed and tested by Figliolini et al. (2020), while a general equation matrix for different mechanisms is in Figliolini et al. (2021). Instead, a small workspace and high rigidity are typical of parallel robots, as in Figliolini et al. (2017).

In this paper, the kinematic synthesis of a tendon-driven 4R planar robotic arm has been developed, in order to reach a given target point within the working area, as well as, to move inside a narrow environment in order to get a given configuration of the robotic arm, which is chosen inside this environment properly.

A. Kecskeméthy and V. Parenti-Castelli (Eds.): ROMANSY 2022, CISM 606, pp. 238–245, 2022.
https://doi.org/10.1007/978-3-031-06409-8_25

2 Tendon-Driven 4R Planar Robotic Arm

A tendon-driven 4R planar robotic arm can be considered an open kinematic chain with four links that are connected each other in series by revolute joints. This kinematic chain has 4 d.o.f.s, which can be operated by means of 4 independent actuators. Each actuator is usually installed far away from the actuated joints. Nevertheless, a suitable transmission system is required to transmit the motion from the actuators to the corresponding joints. This transmission system can be designed by using wires, chains, belts and timing belts, epicyclic gear trains and sprocket chains. From a kinematic point of view these mechanical devices can be considered equivalent among them according to a suitable design.

Figure 1 shows an example of tendon-driven mechanism with 4-d.o.f.s, where both elements of parallel and cross types are connected to form a serial kinematic chain. These elements are equivalent by a kinematic point of view to a pair of internal gears (parallel-type) or external gears (cross-type) and they are composed by a rigid link and two pulleys that are connected by the tendon. Thus, one has

$$R_j\theta_{j,k} = \pm R_{j+1}\theta_{j+1,k} \tag{1}$$

where $\theta_{j,k}$ and $\theta_{j+1,k}$ are the relative rotations of the pulleys j and j+1 of radii R_j and R_{j+1} with respect to the link k. The sign of Eq. (1) is determined by the rotation of the tendon, which is positive for the parallel-type and negative for the cross-type.

Moreover, the oriented angles of the relative rotations can be expressed as

$$\theta_{j,j+1} = \theta_{j,k} - \theta_{j+1,k} \tag{2}$$

In particular, links 1, 2 and 3 are connected in series to shape an open-loop kinematic chain, where 0 is the fixed frame and pulley 4 ≡ j+3 is the end-effector. The rotation of the base pulley j can be related to that of pulley j+3 by means of the oriented angles

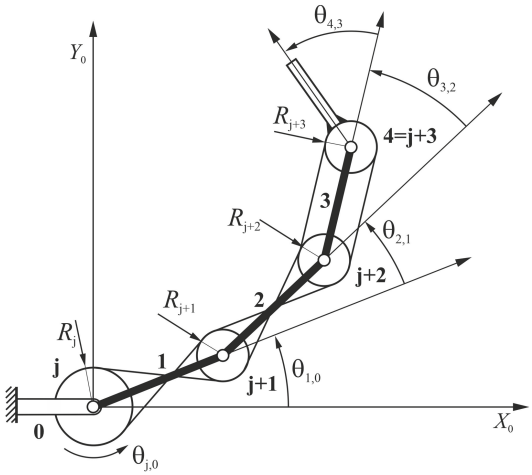

Fig. 1. Example of tendon-driven mechanism with 4-d.o.f.s.

$\theta_{1,0}$, $\theta_{2,1}$, $\theta_{3,2}$ and $\theta_{4,3}$ by which the position equation can be obtained by considering the three kinematic elements of cross and parallel-type, (j, j+1, 1), (j+1, j+2, 2) and (j+2, j+3, 4) respectively, the first two terms denoting the pulleys and third one, their connecting link. Thus, one has

$$R_j\theta_{j,1} = -R_{j+1}\theta_{j+1,1} \quad \theta_{j,0} = \theta_{1,0} + \theta_{j,1} \tag{3}$$

$$R_{j+1}\theta_{j+1,2} = -R_{j+2}\theta_{j+2,2} \quad \theta_{j+1,1} = \theta_{j+1,2} + \theta_{2,1} \tag{4}$$

$$R_{j+2}\theta_{j+2,3} = R_{j+3}\theta_{j+3,3} \quad \theta_{j+2,2} = \theta_{j+2,3} + \theta_{3,2} \tag{5}$$

which give the remote actuation angle $\theta_{j,0}$ of the base pulley j in the form

$$\theta_{j,0} = \theta_{1,0} - \frac{R_{j+1}}{R_j}\theta_{2,1} + \frac{R_{j+2}}{R_j}\theta_{3,2} + \frac{R_{j+3}}{R_j}\theta_{4,3}. \tag{6}$$

The example of Fig. 1 can be generalized to any combination of parallel and cross-type elements by

$$\theta_{j,0} = \theta_{1,0} \pm \frac{R_{j+1}}{R_j}\theta_{2,1} \pm \frac{R_{j+2}}{R_j}\theta_{3,2} \pm \ldots \pm \frac{R_{j+(m-1)}}{R_j}\theta_{m,m-1} \tag{7}$$

where m denotes the number of links of the open-loop kinematic chain.

Therefore, applying Eq. (7) to the planar tendon-driven 4R robotic arm of Fig. 2, one has, in matrix form

$$\begin{bmatrix} \theta_{1,0} \\ \theta_{5,0} \\ \theta_{6,0} \\ \theta_{7,0} \end{bmatrix} = \begin{bmatrix} 1 & 0 & 0 & 0 \\ 1 & \frac{R_8}{R_7} & 0 & 0 \\ 1 & \frac{R_4}{R_6} & \frac{R_4R_{10}}{R_6R_6} & 0 \\ 1 & \frac{R_2}{R_7} & \frac{R_2R_9}{R_7R_7} & \frac{R_2R_9R_3}{R_7R_7R_7} \end{bmatrix} \begin{bmatrix} \theta_{1,0} \\ \theta_{2,1} \\ \theta_{3,2} \\ \theta_{4,3} \end{bmatrix} \tag{8}$$

which gives a lower triangular matrix of coefficients, when all pulleys have the same radius. Figure 2a shows the kinematic chain and Fig. 2b is related to a kinematic sketch to formulate the inverse kinematics for the remote actuation.

The kinematic synthesis of the proposed 4R planar robotic arm has been developed by superposing three tendon-driven kinematic chains, in order to operate by a remote actuation, the last three links 2, 3, and 4, since the link 1 is actuated directly, where L_1, L_2, L_3 and L_4 are the link lengths, while $\theta_{1,0}$, $\theta_{2,1}$, $\theta_{3,2}$ and $\theta_{4,3}$ are the variable joint angles. Thus, for any assigned target point P with respect to the fixed frame OX_0Y_0, the absolute oriented angles θ_1, θ_2, θ_3 and θ_4 of links 1, 2, 3 and 4 of the 4R planar robotic arm, are computed by applying the inverse kinematics.

The corresponding equations are non-linear and can be obtained by the direct kinematics, which is expressed through the Cartesian coordinates of point P, as

$$x_P = L_1\cos\theta_1 + L_2\cos\theta_2 + L_3\cos\theta_3 + L_4\cos\theta_4 \tag{9}$$

$$y_P = L_1\sin\theta_1 + L_2\sin\theta_2 + L_3\sin\theta_3 + L_4\sin\theta_4 \tag{10}$$

Moreover, the proposed 4R planar robotic arm is redundant and thus, provided of 4 d.o.f.s, which means to have four independent parameters, i.e. θ_1, θ_2, θ_3 and θ_4.

Consequently, in order to reduce the number of unknowns, the sketch of Fig. 2b has been assumed, where all links have the same length, the first link is supposed to be oriented toward the target point P and the remaining four-bar linkage is supposed to take the shape of an isosceles trapezoid. Thus, one has

$$\theta_3 = \theta_1 = \tan^{-1}\left(\frac{y_P}{x_P}\right) \tag{11}$$

while the angles θ_2 and θ_4 are obtained by applying the well-known loop-closure equation to the isosceles-trapezoidal four-bar linkage of Fig. 2b by giving

$$\theta_2 = \tan^{-1}\left(\frac{-D + \sigma\sqrt{D^2 + C^2 - E^2}}{E - C}\right) \tag{12}$$

$$\theta_4 = \tan^{-1}\left(\frac{B - L_2 \sin\theta_2}{A - L_2 \cos\theta_2}\right) \tag{13}$$

where σ is equal to ±1 according to the particular assembly mode of the four-bar linkage and the coefficients *A, B, C, D* and *E* are expressed as follows

$$A = x_P - L_1 \cos\theta_1 - L_3 \cos\theta_3, \quad B = y_P - L_1 \sin\theta_1 - L_3 \sin\theta_3 \tag{14}$$

$$C = -2AL_2, \quad D = -2BL_2, \quad E = A^2 + B^2 + L_2^2 - L_4^2 \tag{15}$$

3 Simulations and Validation

The kinematic performances of the designed tendon-driven 4R planar robotic arm have been validated by means of different significant simulations, which have been carried out by implementing in Matlab the proposed inverse kinematic algorithm, along with the matrix Eq. (8), which expresses the remote actuation angles, as function of the joint angles.

In particular, two different conditions have been considered for validation purposes, which are devoted to reach different target points that are chosen freely in the working area of the robotic arm and to move inside a narrow environment in order to reach a given configuration by avoiding any boundary collision.

Thus, supposing all pulleys of Fig. 2a having the same radius and the links length $L_1 = L_2 = L_3 = L_4$ equal to $10u$ with u the unit length, when the Cartesian coordinates of the target point P (x_P, y_P) are given, the remote actuation angles can be calculated as function of the absolute joint angles.

In particular, referring to Fig. 2a, link 4 that is attached to pulley 3 is remotely driven by pulley 5 because of three kinematic elements of parallel-type, where pulleys 2 and 9 are idle on their axes. Link 4 rotates of the same angle of pulley 5.

Similarly, link 3 is remotely driven by pulley 6, because of two kinematic elements of parallel-type, where pulley 4 is idle and pulley 8 is attached to link 2. Thus, link 3

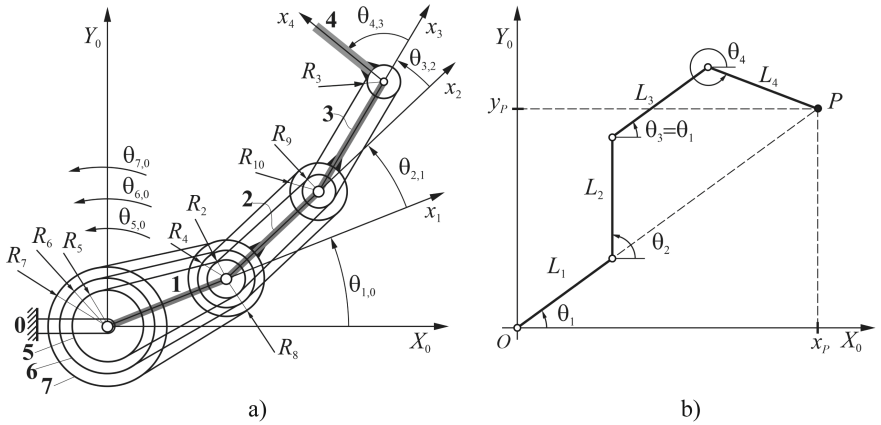

Fig. 2. Tendon-Driven 4R planar robotic arm: a) Kinematic chain; b) Kinematic sketch

rotates of the same angle of pulley 6 and again, the link 2 is attached to pulley 8 and remotely driven by pulley 7, because of a kinematic element of parallel-type. Finally, link 1 is driven directly around its fixed axis.

The movements of this tendon-driven 4R planar robotic arm can be coupled, because the rotation of any link generates the translation of the successive part of the robotic arm and this characterize the proposed design.

For example, the rotation of link 1 gives the translation of links 2, 3 and 4, which are moved as a unique rigid body, while the rotation of link 2 gives the translation of links 3 and 4. Thus, the last link 4 is pure rotated, because there is not any successive link.

The simulations have been developed by considering each link i as actuated by a single motor M_i for $i = 1, 2, 3, 4$, which are installed on each driving pulley. In order to validate the proposed algorithm, along with the capability and functionality of the designed tendon-driven 4R planar robotic arm, two particular operating conditions have been considered, such as, to reach different target points that are chosen freely in the working area and to move inside a narrow environment in order to reach a given configuration by avoiding any boundary collision.

Referring to Fig. 3, the first operating condition has been simulated to reach different target points that are indicated by P_i for $i = 1, 2, 3, 4$, which corresponding configurations of the tendon-driven 4R planar robotic arm allowed the validation of the proposed algorithm, according to the sketch of Fig. 2b. Moreover, the rotations of motors M_i for $i = 1, 2, 3, 4$ are also shown in each figure.

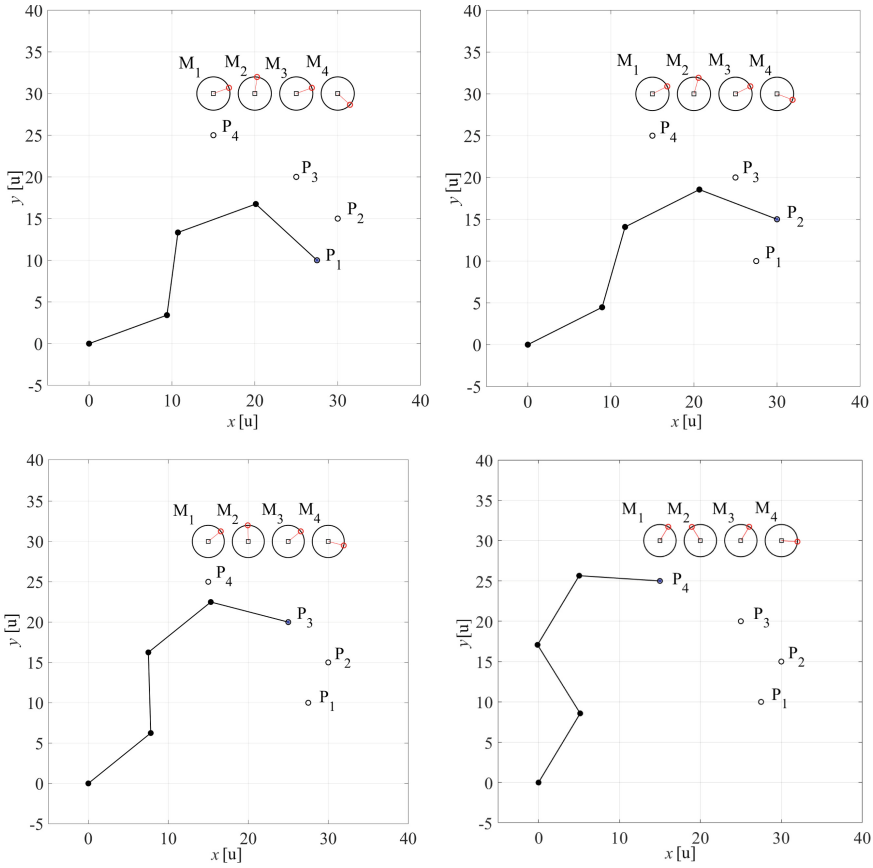

Fig. 3. Simulation for given target points (where u is the unit length).

Referring to Fig. 4, the second operating condition has been simulated to move the robotic arm inside a narrow environment in order to reach a given configuration by avoiding any boundary collision.

In particular, points P_i for i = 1, 2, 3, 4 have been chosen inside the given narrow environment, in order to reach the final configuration of the robotic arm, according to a specific path, which lets to calculate the absolute angles of each segment.

Thus, the path is discretized and the intermediate absolute angles are calculated to determine the successive positions of each link of the robotic arm during its motion. In particular, the discretization between two consecutive points has been calculated by assuming a step equal to 1, while the rotation angles of the corresponding driving pulleys have been obtained by using Eq. (8).

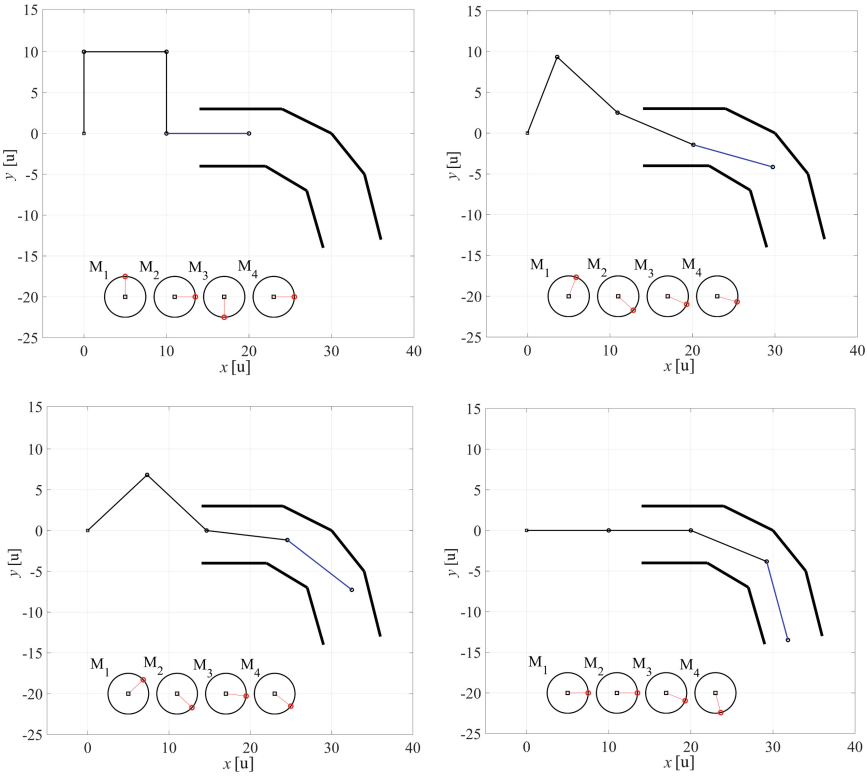

Fig. 4. Second simulation by given a set of points (where *u* is the unit length).

4 Conclusions

In this paper, the kinematic synthesis of a tendon-driven 4R planar robotic arm with 4 d.o.f.s and thus, two times redundant, has been developed by superposing three tendon-driven kinematic chains, in order to operate each link by means of a suitable remote actuation. Moreover, a specific algorithm has been formulated to reach a given target point within the working area and to move inside a narrow environment. Significant examples have allowed the validation of the proposed design of the tendon-driven 4R planar robotic arm and the related algorithm for two different operating conditions.

References

Figliolini, G., Ceccarelli, M.: A motion analysis for one D.O.F. anthropomorphic finger mechanism. In: CD Proceedings of the 25th ASME Biennial Mechanisms Conference (DETC'98), Atlanta, USA, DETC98/MECH-5985 (1998)

Figliolini, G., et al.: Mechatronic design of a robotic arm to remove skins by wine fermentation tanks. In: Carcaterra, A., Paolone, A., Graziani, G. (eds.) AIMETA 2019. LNME, pp. 271–277. Springer, Cham (2020). https://doi.org/10.1007/978-3-030-41057-5_22

Figliolini, G., Lanni, C., Di Donato, L., Melloni, R., Bacchetta, A.P.: Kinematic synthesis of a tendon-driven robotic arm. In: Niola, V., Gasparetto, A. (eds.) IFToMM ITALY 2020. MMS, vol. 91, pp. 386–393. Springer, Cham (2021). https://doi.org/10.1007/978-3-030-55807-9_44

Figliolini, G., Lanni, C., Rea, P., Gallinelli, T.: Mechatronic design and control of a 3-RPS parallel manipulator. In: Ferraresi, C., Quaglia, G. (eds.) RAAD 2017. MMS, vol. 49, pp. 74–81. Springer, Cham (2018). https://doi.org/10.1007/978-3-319-61276-8_9

Krovi, V., Ananthasuresh, G.K., Kumar, V.: Kinematic and kinetostatic synthesis of planar coupled serial chain mechanisms. ASME J. Mech. Des. **124**(2), 301–312 (2002)

Londi, F., Pennestrì, E., Valentini, P.P., Vita, L.: Control and virtual reality simulation of tendon driven mechanisms. Multibody Sys.Dyn. **12**(2), 133–145 (2004)

Okur, B., Zergeroglu, E., Tatlicioglu, E.: Nonlinear control of tendon driven robot manipulators: elimination of actuator side position measurements. In: 54th IEEE Annual Conference on Decision and Control (CDC), 15–18 December 2015, Osaka (Japan), pp. 1491–1496 (2015)

Ozawa, R., Kobayashi, H., Hashirii, K.: Analysis, classification, and design of tendon-driven mechanisms. IEEE Trans. Rob. **30**(2), 396–410 (2014)

Tsai, L.-W.: Robot Analysis and Design: The Mechanics of Serial and Parallel Manipulators, 1st edn. Wiley, New York (1999)

Tsai, L.-W., Lee, J.-J.: Kinematic analysis of tendon-driven robotic mechanisms using graph theory. J. Mech. Trans. Autom. Des. **111**(1), 59–65 (1989)

Tsai, L.W.: Design of tendon-driven manipulators. ASME J. Mech. Des. **117**(B), 80–86 (1995)

Uyguroglu, M., Demirel, H.: Kinematic analysis of tendon-driven robotic mechanisms using oriented graphs. Acta Mech. **182**, 265–277 (2006)